Universiteit
Leiden
The Netherlands

The role and analysis of molecular systems in electrocatalysis

Dijk, B. van

Citation
Dijk, B. van. (2021, March 10). *The role and analysis of molecular systems in electrocatalysis*. Retrieved from https://hdl.handle.net/1887/3151631

Version:	Publisher's Version
License:	Licence agreement concerning inclusion of doctoral thesis in the Institutional Repository of the University of Leiden
Downloaded from:	https://hdl.handle.net/1887/3151631

Note: To cite this publication please use the final published version (if applicable).

Cover Page

Universiteit Leiden

The handle https://hdl.handle.net/1887/3151631 holds various files of this Leiden University dissertation.

Author: Dijk, B. van
Title: The role and analysis of molecular systems in electrocatalysis
Issue Date: 2021-03-10

Chapter 1

Introduction to the role and analysis of molecular systems as electrochemical catalysts

Efficient water splitting and fuel cell technology will greatly determine the success of the energy transition from fossil fuels to renewable energy such as solar and wind power. This introductory chapter discusses the role of molecular complexes as electrocatalysts in these reactions. The high tunability of the ligands of these complexes allows for structural diversity. Thereby, these complexes can be used as structural mimics to unravel the catalytic mechanisms of enzymes, or be used as catalysts designed by taking inspiration from the active site of these enzymes. In addition, structure–activity studies can be performed with molecular systems giving direct information about what factors improve the rate determining step and catalysis as a whole. These factors include the electronic withdrawing or donating effect of the ligand, steric bulk or the absence thereof, or the importance of proton coupled electron transfer steps that avoid charge build-up. However, the major drawback of molecular complexes is the stability. Several degradation pathways are discussed and their impact on catalysis. In cases where the parent complexes has degraded, the ligand can still have an influence. Beneficial concepts from homo- and heterogeneous catalysis could then lead to new strategies to improve catalysts. Lastly, the analysis of molecular systems by various electrochemical techniques is discussed which can give information regarding the kinetics, product distribution, and stability of the complexes. In addition, any pitfalls accompanying the use of these techniques are discussed as these can easily lead to over- or misinterpretation. This thesis discusses various molecular complexes for O_2 reduction and H_2O oxidation and will show how the techniques, introduced in this chapter, allow for proper characterization of the active species, identify any decomposition pathways and aid in structure–activity relationship studies.

1.1 The role of electrochemistry in renewable energy

1.1.1 H_2O oxidation to O_2 and *vice versa*

On an almost daily basis, the news confronts us with the global climate crisis. The large scale use and dependence on fossil fuels is leading to global temperature rises with many negative consequences such as climate change and rising seawater levels.[1] Currently, a large share of the renewable energy is consisting of electricity generated from solar and wind power. However, these energy sources are not available 24 hours a day. Diminishing the intermittency effects of these energy sources by large scale energy storage is still a major challenge. One solution, mostly beneficial for short distance mobility, is electricity storage in batteries. However, batteries have a low energy density implicating that the ratio of stored energy to weight is low. For applications that require a high amount of energy storage, such as long and large scale transit, batteries that can store enough energy will simply be too heavy.[2] H_2 is often chosen as an energy carrier in those cases. Even though the energy density of H_2 is lower than that of organic fossil- or biofuels,[2] producing H_2 is in principle as simple as running a current through water with electrolyte. It is not so surprising that water electrolysis has been known since 1789.[3] In detail, water electrolysis is the splitting of water in H_2 and O_2 according to half reactions in Equations 1.1 and 1.2.

$E^\circ = 0.00\ V$ $\quad 4H^+ + 4e^- \rightleftharpoons 2H_2$ **Eqn. 1.1**

$E^\circ = 1.229\ V$[4] $\quad O_2 + 4H^+ + 4e^- \rightleftharpoons 2H_2O$ **Eqn. 1.2**

The equilibrium potential (E°) is the potential at which the reaction is at the thermodynamic equilibrium. At more positive potentials, the oxidation (H_2 to H^+/ H_2O to O_2) is favored and at negative potentials the reduction (H^+ to H_2/O_2 to H_2O). In principle, 1.229 V is required to oxidize water to H_2 and O_2 as this is the difference in E° of Equations 1.1 and 1.2. However, there is always a kinetic barrier, the activation energy, that requires an additional energy input. For that reason, catalysis generally does not occur at the equilibrium potential. The potential difference between the potential that needs to be applied for catalysis to occur and the equilibrium potential is also called the overpotential (η). A higher energy barrier will result in a higher η. Whereas the E° is often well defined, the actual potential where catalysis starts (also called the onset potential) is not. Often, it is defined as the

potential where a pre-determined magnitude of current is reached, but this gives rise to discrepancies in the definition of onset potentials between different studies.

The extra energy input required due to the overpotential can be considered as energy loss. A low overpotential is therefore highly desired. The overpotential is linked to the height of the activation energy barrier of the reaction. Catalysts are able to lower this barrier by binding the substrate and thereby providing a new thermodynamic route for the making and breaking of bonds. These routes have steps with lower activation barriers than the uncatalyzed reaction. Not every catalyst will lower the energy barrier of any reaction. The binding strength between the catalyst and the substrate is of importance. The Sabatier principle is a general description of the ideal properties of a catalyst. It states that a catalyst that binds the substrate too strongly, will not be able to release intermediates or products. On the other hand, if the substrate has a very weak interaction with the catalyst, no reaction might occur. The ideal catalyst is in the middle of that. As each possible catalyst material has a different binding strength with a substrate, each catalytic reaction can have a unique ideal catalyst that lowers the energy barriers most efficiently for that particular reaction.

Two different catalysts are used for the electrochemical production of H_2 by polymer electrolyte membrane electrolyzers. For the hydrogen evolution reaction (HER) (reductive part of Eqn. 1.1), state of the art catalysts are composed of platinum nanoparticles dispersed on carbon black supports. These achieve outstanding current densities at a low overpotential.[5, 6] Platinum catalysts carry out both the HER and the H_2 oxidation reaction (HOR) close to the equilibrium potential with high forward and backward rates. When a catalyst performs both the oxidation and the reduction of a catalytic reaction with barely any overpotential (reversible electrocatalysis), it is considered as an ideal catalyst. In terms of minimal energy losses, platinum can be considered as ideal catalyst for the HER (and HOR). In fact, the OER (O_2 evolution reaction, Eqn. 1.2) is the bottleneck of electrolyzers. Currently, iridium oxide achieves the lowest overpotentials with a considerable OER rate, but is not an ideal catalyst such as Pt is for HER since there is significant energy loss due to the overpotential at which iridium oxide has to operate.[6] In addition, iridium is, along with platinum, rhodium, and palladium, one of the most scarce metals on earth (Figure 1.1).[7] Moreover, the even distribution in the earth's crust limits the amount of Ir-rich sources.[8] Therefore, most research has focused on increasing the active surface area so that iridium loadings can be reduced.[6] To date, the research goals are finding better dispersing supports that are stable under oxidative conditions and/or better catalysts preferably using less scarce metals.

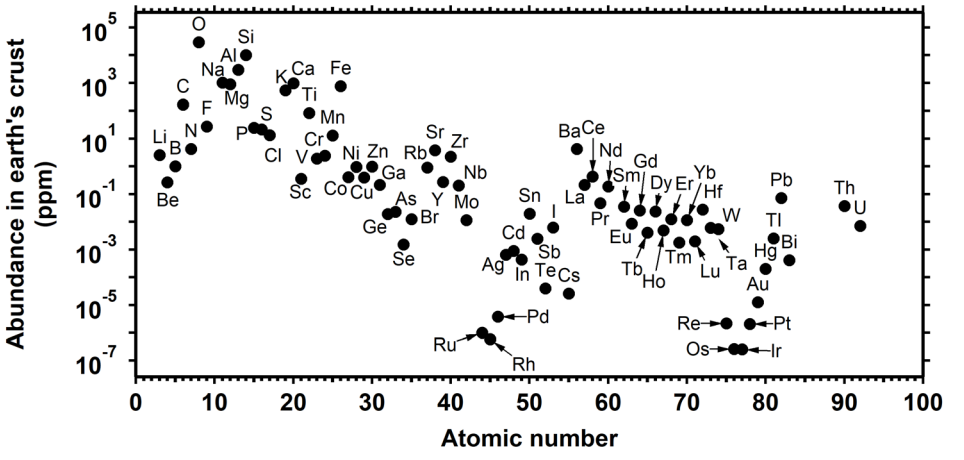

Figure 1.1. Average natural abundance of elements in the earth's crust.[7] The abundance (ppm in weight) was corrected for the atomic weight of the elements.

Apart from producing H_2, electrochemistry is important for utilizing the energy that is released when H_2 is oxidized. This is achieved in fuel cells. Here, the HOR at the anode and the O_2 reduction reaction (ORR) at the cathode are performed resulting in an electric current. Obviously, highly dispersed Pt catalysts are used for the HOR since it is the ideal catalyst. Again, it is the half reaction of Eqn. 1.2 that is the bottleneck. The most energy efficient catalyst for ORR is actually Pt as well.[9] Nonetheless, platinum catalysts cannot operate at the thermodynamic potential of 1.23 V thus reducing the efficiency significantly.[10] Scaling relations prevent predominantly the optimization of heterogeneous catalysts such as platinum. In brief, scaling relations suggest that catalyst binding strength of intermediates is dependent on each other.[11, 12] As a consequence, optimizations of the binding strength for a specific intermediate according to Sabatier's principle, will negatively affect the binding strength of another intermediate. Therefore, most heterogeneous catalyst development is only focused on mass transport optimization to reduce catalyst loadings.[13] To illustrate the challenge that is faced in reducing catalyst loadings, the requirements for the replacement of fossil fuel driven cars by fuel cell driven cars is given as example. Currently, at least 50 g of platinum for a medium-sized vehicle would be required to be able to power it via a fuel cell.[14] Due to the scarcity and costs associated with that amount of platinum, it is estimated that there must be a more than 8 fold reduction of catalyst (maximum of 6 g per vehicle) in order to have feasible large scale fuel cell car production.[15] In this scenario, only medium-sized vehicles are considered. One can imagine that replacing all fossil fuel

driven processes by fuel cells is basically impossible considering the scarcity and costs of platinum. Thus, the need for intrinsically more efficient catalysts for both electrolyzers and fuel cells is high.

1.1.2 H_2O_2 production from O_2

The ORR is generally considered and investigated as the reaction in Eqn. 1.2: the full 4 electron reduction of O_2 to H_2O. However, the 2 electron reduction to H_2O_2 is possible as well (Eqn. 1.3). For fuel cells, H_2O_2 as the product of O_2 reduction is undesired since it is highly corrosive. Moreover, the E° of O_2 to H_2O_2 is 0.695 V (Equation 1.3), which is lower than that of the full 4 electron reduction to water (1.229 V).[4] Thus, the theoretical maximum output potential of a fuel cell, when H_2O_2 is the product, is lowered to 0.695 V instead of 1.229 V. Nevertheless, H_2O_2 is a valuable product. In fact, H_2O_2 is a bulk chemical that is used in applications varying from organic synthesis,[16] waste water treatment,[17, 18] to, most importantly, bleaching of wood or paper pulp.[19, 20] H_2O_2 is a very environmentally friendly reagent following that only H_2O or O_2 are generated as waste. This is in sharp contrast to the production method of H_2O_2. The anthraquinone process is responsible for over 90% of the global H_2O_2 production.[21, 22] This process relies on the reduction of O_2 with H_2 by anthraquinones. These redox mediators have limited life cycles and have to operate in organic solvent mixtures. Obtaining highly concentrated, pure aqueous H_2O_2 solutions requires energy intensive purification steps that increase the waste and costs significantly. Using the electrochemical O_2 to H_2O_2 reduction in aqueous media with electricity from renewable sources is a worthwhile alternative that can also be used as "on-site" production method.

$$E° = 0.695\ V \qquad O_2 + 2H^+ + 2e^- \rightleftharpoons H_2O_2 \qquad \textbf{Eqn. 1.3}$$

The electrocatalytic reduction of O_2 to H_2O_2 can be carried out by various catalysts such as metal alloys[23-26] or carbon based electrodes.[26-35] The latter category includes electrodes such as pyrolytic graphite (PG) and glassy carbon (GC) that have an intrinsic high selectivity for the 2 electron reduction of O_2 to H_2O_2. Yet, defects and heteroatoms (such as nitrogen), introduced via *in-situ* electrode degradation, can change the selectivity towards the 4 electron reduction. Also, the overpotential is still significantly high. Therefore, research into selective H_2O_2 producing electrocatalysts is of high interest, especially as such a production process would be suitable for on-demand and on-site production of H_2O_2.

1.1.3 Homogeneous *versus* heterogeneous catalysis

Overall, the reactions in Equations 1.2 and 1.3 will play a very important role in a sustainable energy infrastructure and an important contribution lies in the field of electrocatalysis. As will be elaborated, this thesis is focused on molecular complexes. Often, these are seen as homogeneous catalysts. A generalized difference between homo- and heterogeneous catalysts is whether the catalyst is in the same phase (homogeneous), or in a different phase (heterogeneous) as the reactants. Interestingly, electrocatalysis will always require an electrode which is inherently in a different phase (solid) than the substrate such as O_2 (gas) or H_2O (liquid). Heterogeneous electrocatalysts are often either the electrode material itself, or a deposited catalyst layer on a conductive substrate such as GC or a metal. In this perspective, homogeneous catalysts are performing electrocatalysis in the electrolyte itself, but only close to the surface of an (heterogeneous) electrode where these are able to exchange electrons. They might even have to adsorb on the electrode for that purpose. For that reason, concepts from heterogeneous catalysis such as surface area, diffusion constants and mass-transport become important. Moreover, the bulk of the solution is not (entirely) involved in catalysis which is all in contrast with classic homogeneous catalysis. Also, molecular catalysts might have different activity and/or selectivity when they are heterogenized (attached to the electrode surface). An example are Fe^{II} porphyrins that perform electrochemical O_2 reduction both homogeneously and, when adsorbed on the electrode surface, heterogeneously.[36] A small difference in selectivity for H_2O_2 production was observed which was ascribed to faster formation and protonation of the Fe^{II}–O_2 adduct when the Fe porphyrin was adsorbed on the electrode. In some cases, molecular catalysts can have such high affinity with the electrode surface that homogeneous electrocatalysis is not possible. An example are planar cobalt porphyrins that adsorb readily and irreversibly on the surface of glassy carbon electrodes.[37] Homogeneous electrocatalysis thus borders heterogeneous catalysis. Various electrochemical techniques derived from that latter field can be (partially) applied to homogeneous electrocatalysis. *Vice versa*, lessons from homogeneous catalysis, such as structure–activity correlations and mechanistic studies, can enhance knowledge about catalyst improvements and perhaps help to uncover new and improved catalytic cycles.

The rest of the introduction will introduce the concepts of electrocatalysis by molecular complexes, examples of structure–activity relationships, pitfalls that are related to catalyst degradation and the use of electrochemical techniques to study kinetics, product distribution and catalyst stability.

1.2 Molecular complexes for redox catalysis

1.2.1 Advantages of molecular complexes in redox catalysis

Molecular complexes are generally highly customizable by ligand modifications resulting in interesting scaffolds for studying catalytic reactions.[38-41] Even though the aforementioned scaling relationships must apply to homogeneous catalysis as well,[42] ligand modifications can still greatly enhance the efficiency of catalysts, but also provide mechanistic insight. One use of complexes is as structural mimic for enzymatic active sites, thereby offering insight and spectroscopic reference for the *modus operandi* of enzymes and perhaps mimic the enzymatic reactivity in catalysis. Another great use of molecular complexes is the ability for systematic structural modifications such as placing electron donating or withdrawing substituents on the backbone of the ligand or the synthesis of multi-metallic systems that both give vital clues to their influence on the rate determining step. In that way, identifying factors that improve rate, but also unraveling the catalytic mechanism can become straightforward. Yet, the structural diversity can come with a price. Ligand oxidation by reactive intermediates can result in the loss of the ligand and/or electrodeposition. These problems will not always be clear in advance and thus various spectroscopic and electrochemical techniques must be employed to identify what is initiating the catalytic activity: the parent complex or, in fact, the degraded (and deposited) complex. At first sight, the latter case seems highly undesirable. Yet, ligand effects may still play a role and could eventually be put to use showcasing where benefits from homo- and heterogeneous catalysis can be combined.

1.2.2 Molecular complexes as structural mimics of enzymes

One of the uses of molecular complexes is as structural mimic for enzymatic active sites. For example, molecular model systems can be a spectroscopic reference to determine the structure of the active site. Likewise, the geometry and coordination environment of the enzyme can serve as inspiration to design catalysts with similar reactivity and activity. A group of enzymes often used as inspiration for performing the ORR efficiently are multi-copper oxidases (MCOs). The active site of these MCOs contains copper clusters including type 1 (“blue copper”), type 2 (“normal copper”) and/or type 3 (dinuclear) copper cores.[43] MCO’s reduce O_2 to H_2O to be able to oxidize a substrate. One of the most profound examples of an MCO is laccase that has a trinuclear copper active site that reduces O_2 (Figure 1.2). Immobilization studies found that not only O_2 reduction, but also H_2O oxidation could be performed close to the equilibrium potential of 1.23 V.[44-51] Pathways that are inaccessible to

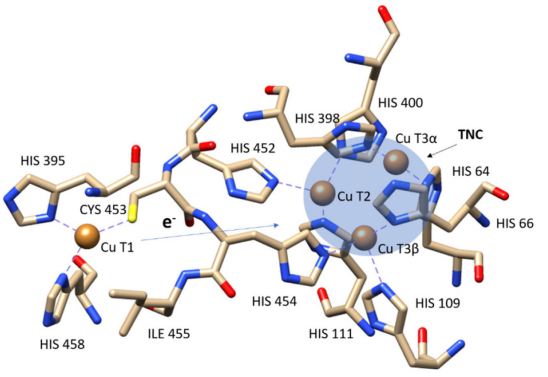

Figure 1.2. Illustration of the active sites of laccase showing the T1 and T2/T3 copper sites. Adapted from Wasak *et al.*[53] (CC BY 4.0 license)

traditional heterogeneous catalysts such as the destabilization of water by carboxylate groups from the second coordination sphere and the irreversible formation of a triangular μ_3-O_2 bond that facilitates fast electron transfer are suggested to be responsible for this low overpotential.[52]

Long term stability and the low number of active sites are drawbacks of enzymatic catalysis hindering direct application in fuel cells.[49-51, 54]. Here, copper complexes that are structural mimics have played a large role to extract spectroscopic information of key intermediates in the activation of oxygen so that these lessons could lead to the design of better electrocatalysts.[55-61] For example, the interconversion of side-on peroxodicopper and bis-μ-oxo dicopper cores in enzymes have been spectroscopically identified by linking the spectroscopy of model copper complexes for which this behavior had been unambiguously proven. Crystallographic studies would not have been able to reveal this dynamic equilibrium.[62] UV-vis, Raman and electronic paramagnetic resonance (EPR) data have been extensively used to character the active site and the intermediates in MCO driven O_2 reduction.

Another enzyme that has sparked interest is the oxygen-evolving complex of Photosystem II. This enzymatic OER catalyst contains a manganese active site. The oxygen-bridged tetranuclear core contains three manganese and one calcium site (Figure 1.3).[63] A simple complex with a di-μ-oxo dimanganese core and terpyridine ligands (Chart 1.1A) was suggested as catalytic mimic since the complex also achieved high oxidation states.[64] However, under electrochemical conditions a tetranuclear complex is formed that is catalytically inactive.[65, 66] Specifically designed tetranuclear Mn_4O_4-cubane clusters (Chart 1.1B) were found to be inactive under homogeneous conditions as well, but with Nafion-assisted immobilization the clusters had water

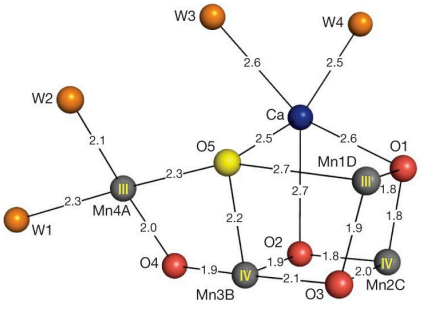

Figure 1.3. Tetranuclear core of the active site of the oxygen evolving complex of Photosystem II. Adapted from Suga *et al.*[63]

oxidation activity.[67] The authors suggested that this could be due to a more efficient distribution of the clusters on the electrode and simultaneous protection from the bulk aqueous electrolyte, though no further investigations to support these hypotheses were conducted.

1.2.3 Mechanistic insight from redox catalysis with sacrificial reagents

The reactivity of most molecular complexes for redox catalysis is studied initially with sacrificial reagents. For water oxidation, cerium(IV) ammonium nitrate (CAN) is often used as sacrificial oxidant which supplies the thermodynamic oxidative power for water oxidation. However, the pH range is limited with CAN

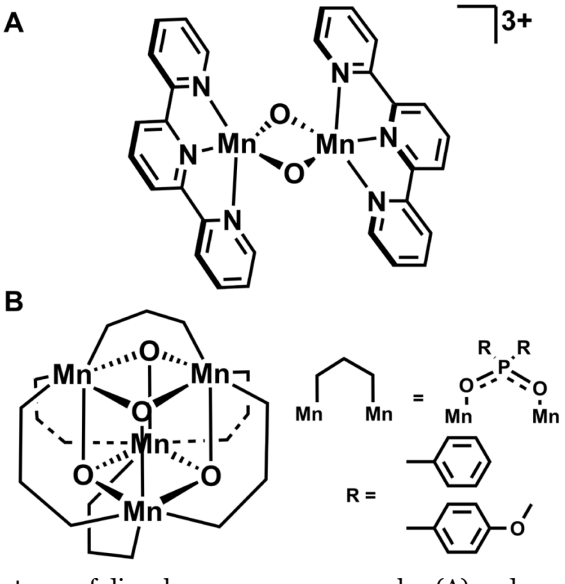

Chart 1.1. The structures of dinuclear manganese complex (A) and a cubane cluster with a Mn_4O_4 core (B) proposed as mimics for the active site of photosystem II.

since it is only stable at low pH.[68] Among other oxidants, sodium periodate is an often used oxidant especially since it can operate at neutral pH as well. One field where the OER has extensively been studied with sacrificial oxidants, is the field of ruthenium based OER that started with the first known molecular water oxidation catalyst (the blue dimer).[69] Often, the ruthenium complexes are studied electrochemically to establish redox potentials, while the catalytic activity is assessed with sacrificial oxidants. The advantage of using oxidants is that, in principle, all catalyst in solution can participate in the reaction. As a result, the turnover number (TON, amount of catalytic cycles per catalyst) and turnover frequency (TOF, TON per time unit) can be easily determined. Moreover, the concentration of Ce^{IV} can be actively tracked by UV-vis allowing for detailed kinetic studies.[70] An important lesson that was learned from ruthenium based OER, was the importance of proton coupled electron transfers (PCET).[71] A PCET step in a catalytic mechanism is the simultaneous transfer of an electron and a proton. The result of a PCET is that there is no net effect on the charge of the active species after oxidation or reduction. Charge build-up is avoided and the redox potentials of higher oxidation states of molecular complexes will be closer together.[72] Ruthenium complexes generally need to reach the high Ru^{V} state to generate a metal-oxo species and can do so by starting with a $Ru^{III}–OH_2$ moiety that can undergo two consecutive PCET steps to a $Ru^{IV}–OH$ and $Ru^{V}=O$ species. Another insight gained from ruthenium based water oxidation chemistry is that there are two mechanisms for O–O bond formation: the water nucleophilic attack or the intermolecular coupling of two metal-oxyl radicals (Scheme 1.1).[73, 74]

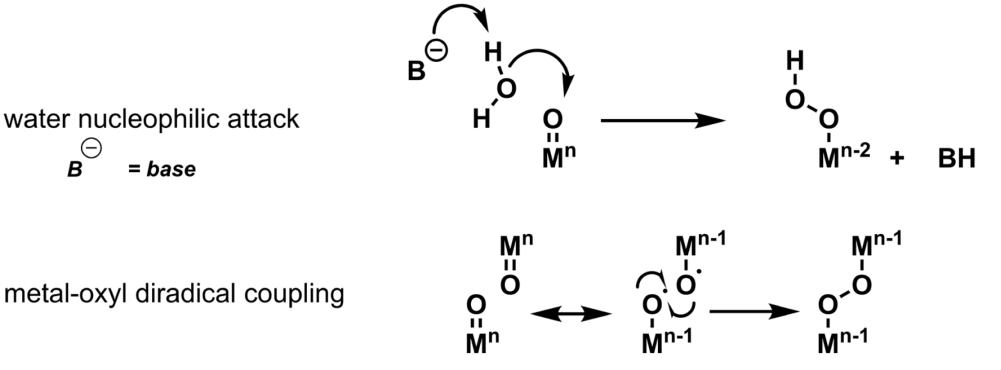

Scheme 1.1. Schematic representation of the water nucleophilic attack or intermolecular coupling of two metal-oxyl radical species.

An important ligand modification that enhanced the activity of ruthenium complexes, is the addition of anionic carboxylate groups on a bipyridine ligand

(Chart 1.2A) that resulted in a distorted octahedral geometry of the complex. That way, a 7-coordinate dinuclear intermediate became more accessible to facilitate O–O bond formation via the metal–oxyl coupling mechanism which in turn increased the turnover frequency for OER significantly.[75] Furthermore, the redox potential for the Ru^{V} species that is required for OER catalysis can, in general, be lowered by various adjustments to the ligand[76] and specifically by introducing electron withdrawing groups.[77-79] In addition, attractive non-covalent interactions of the ligand can also positively impact the rate of water oxidation. However, having electron withdrawing groups will not always improve the OER. For example, a series of terpyridine ruthenium complexes with substituted bipyridine ligands (Chart 1.2B) showed reversed trends as in that electron donating groups improve the catalytic rate.[80]

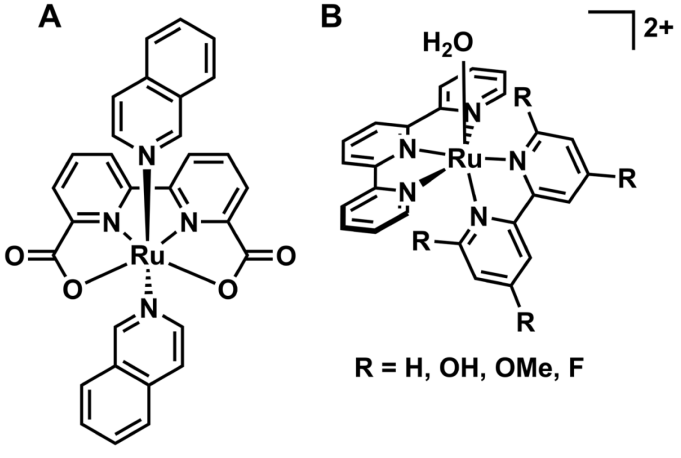

Chart 1.2. Ruthenium complex with dicarboxylate substituents on the bipyridine ligand (A) and ruthenium terpyridine complexes with substituted bipyridine ligands (B).

The ruthenium OER chemistry has laid a good foundation for fast catalysts and mechanistic insight. Nevertheless, results and insight obtained by catalysis with sacrificial oxidants cannot unconditionally be transferred to electrocatalytic conditions. Regularly, electrochemically studied redox potential and catalytic onset potential shifts due to substituent induced electronic differences between complexes are compared to catalytic TOF's derived from sacrificial reagent studies. However, these sacrificial reagents might actually participate in the catalytic cycle,[81] or the oxygen atoms of the nitrate of CAN might be incorporated in the formed O_2 molecule.[82] In the latter case, there is actually no formal water oxidation. Oxygen labeling studies could be used to investigate this possibility, though for sodium periodate this is not possible, since it readily exchanges oxygen atoms with water.[83] In addition, the oxidative potential of these sacrificial reagents is completely

dependent on their concentration according to the Nernst equation and will thus vary uncontrollably during catalysis. To illustrate, at the start of an experiment with CAN there is only cerium (IV) and no cerium (III) present yet. Hence, the potential at the start is, in theory, infinitely high which would translate to an infinite overpotential under electrocatalytic conditions. In addition, care has to be taken into translating results to electrochemical conditions as structure–activity relationships might not prevail. When sacrificial reagents participate in the catalytic mechanism the rate determining step can be different under electrochemical conditions. In some cases, the influence might actually be inversed. A good example is that of a study into Cp* (Cp* = pentamethyl cyclopentadienyl) iridium complexes with tunable carbene ligands (Chart 1.3A).[84] This study reported a clear correlation between electron donating substituents and an enhancement of the catalytic TOF with sacrificial reagents. In contrast, the best performing electrocatalytic system was the unsubstituted complex.

A last word of caution includes the stability of complexes under electrochemical conditions. A series of Cp* iridium picolinate catalysts (Chart 1.3B) previously showed a good correlation between the electron donating ability of the picolinate ligands and the water oxidation activity with sacrificial reagents. Later, electrochemical studies showed that these relationships did not translate to those conditions because of catalyst degradation (see Chapter 2).[85, 86] Sacrificial reagents are often, especially in the field of OER catalysis, used to easily study the catalytic performance of molecular complexes. However, these examples show that without actual electrocatalytic studies, one to one translation of the results of sacrificial reagent driven catalysis to electrocatalytic conditions is not possible.

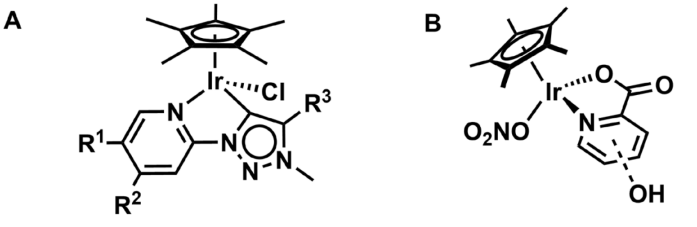

Chart 1.3. The structures of the carbene iridium complexes (A) and iridium picolinate complexes (B) used for comparative sacrificial and electrochemical structure–activity studies.

1.2.1 Structure–activity relationships in electrocatalysis

Structure–activity relationships (SAR's) are a powerful tool to gain mechanistic insight and to design better catalysts. The ligand framework of molecular complexes can be tuned in such a way that the geometry and/or the electronic properties of a complex are altered. In the previous section, SAR's with sacrificial reagents have been discussed, but SAR's can be found under electrocatalytic conditions as well. Often, the equilibrium redox potential of the metal (the $E_{1/2}$) has a clear relationship, especially when substituents, that have an electron donating or withdrawing effect, are placed on the ligand. This electronic effect can be described by the Hammett parameter. Originally, this parameter was derived for the rate of reactions involving substituted aromatic compounds, such as esterification/hydrolysis and bromination, but also the pK_a of benzoic acids and phenols.[87, 88] For electrocatalysis, the Hammett parameter can correlate to the $E_{1/2}$ of the complex or even to the catalytic rate and/or onset potential. Even in cases without clear correlations, structural diversity can give clues regarding the rate determining step.

One example of SAR studies for O_2 reduction encompasses closely related bis- and tris-pyridyl Cu^{II} complexes (Chart 1.4A). The difference in linker length between the central amine and pyridine or the number of pyridines (2 or 3) shifted the $E_{1/2}$ of the $Cu^{I/II}$ redox couple. Interestingly, the O_2 reduction rate differed among the complexes, but with no clear relation to the $E_{1/2}$.[89] Another study claimed that substituents on the *ortho*-position of the pyridines had no significant influence on the onset potential for O_2 reduction.[90] A first conclusion was that Cu^{II} to Cu^{I} reduction nor protonation of a superoxo species would be the rate determining step. Of note, this latter study studied these *ortho*-substituted complexes at pH 1 where the pyridines might be protonated and not able to coordinate to copper resulting in free copper ions in the solution. In addition, the lessons learned from this set of ligands cannot be extrapolated to all copper complexes. In contrast to the previously mentioned copper series, linear relationships between the $E_{1/2}$ of the redox couple and the O_2 reduction rate were in fact found for several (substituted) bipyridine and phenanthroline copper complexes (Chart 1.4B). In detail, the half wave potential of the catalytic wave corresponded linearly with the redox couple whereas the rate constant had an inverse correlation with the redox couples.[91] Later, the linear dependence was pinpointed to the electron withdrawing nature and the steric demands of the substituent which both result in a higher half wave potential but lower catalytic rate.[92] For the ORR, cobalt porphyrins had a clear substituent effect on the redox couple (Chart 1.5).[93, 94] More electron donating sulfonate groups *versus*

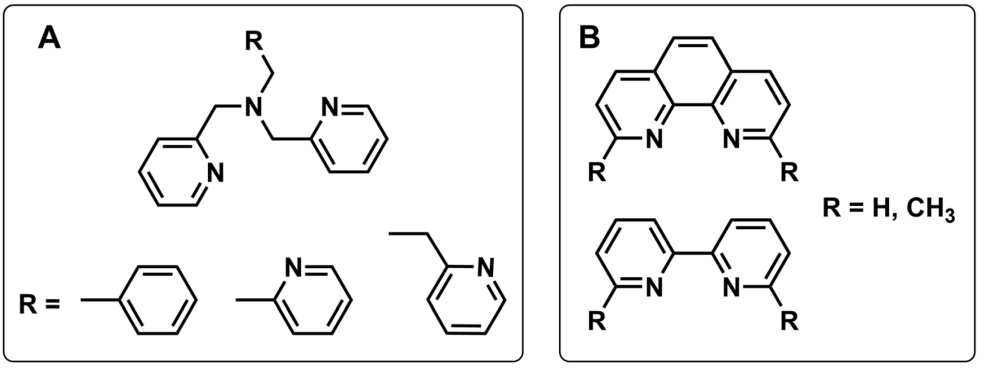

Chart 1.4. Ligands used for the study of Cu^{II} complexes with variable linker length between the pyridine and the central amine, as well as the variable presence of a pyridinic moiety (A) and the structure of the bipyridine and terpyridine ligands (B).

electron withdrawing N-methylpyridine clearly shifted the redox couple to lower potentials. The most interesting observation was that in the case of the N-methylpyridine porphyrins, the $E_{1/2}$ of the redox couple occurred before the catalytic wave whereas the $E_{1/2}$ of the sulfonate substituted porphyrin complex was lower than that of the onset of O_2 reduction. A change of mechanism where O_2 is reduced either by a Co^{I} or a Co^{II} species was proposed and related to a positive shift of the O_2 reduction onset for the latter. Interestingly, these porphyrins are non-planar which prevented adsorption on glassy carbon electrodes as opposed to the earlier discussed planar analogues.[37]

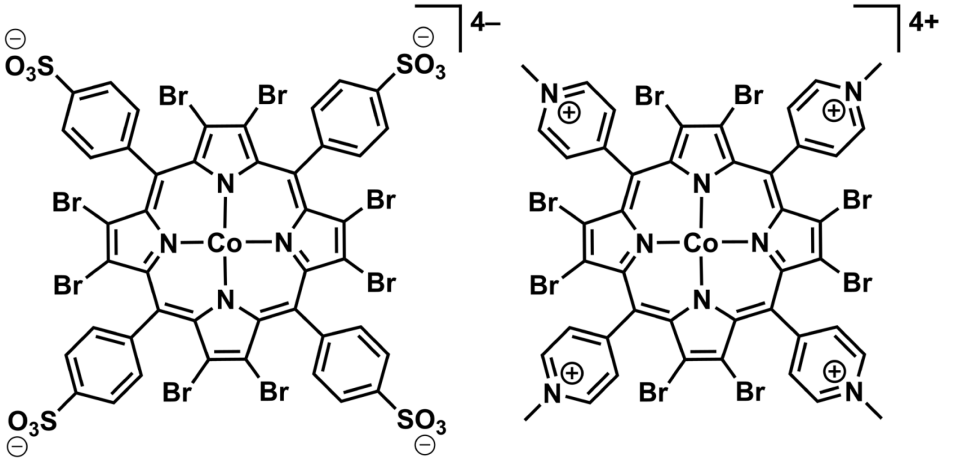

Chart 1.5. The planar cobalt complexes studied for electrochemical O_2 reduction.

The performance of catalysts for electrocatalytic water oxidation can also be boosted with ligand modifications. Electron donating substituents on tetra-anionic tetradentateamidate copper complexes (Chart 1.6A) resulted in a reduction of the overpotential down to 170 mV. Additionally, computational studies suggested that within the catalytic cycle, the ligand stabilizes a peroxo intermediate via hydrogen bonds after O–O bond formation without the presence of a formal metal–O bond.[95] For a series of dinuclear manganese terpyridine complexes (Chart 1.6B), electron donating substituents on the terpyridine resulted in a decrease the $E_{1/2}$ of their respective complexes as well as a decrease of the second order rate constant for the OER. Interestingly, some of the bulkier substituents increased the rate more than expected based on their respective Hammett parameters.[96] However, the $E_{1/2}$ correlated linearly with the catalytic rate constant. Interesting to note here, is that terpyridine based ruthenium complexes actually catalyzed the water oxidation with higher rates with electron donating substituents on the terpyridine backbone.[80]

SAR's under electrocatalytic conditions are not always as straightforward as SAR's from sacrificial reagent studies would predict. Generally, the $E_{1/2}$ of a complex has a good relationship with the electron donating or withdrawing effect of a ligand and might even be correlating to the corresponding Hammett parameter. Interestingly, when the overpotential can be reduced by in- or decreasing the $E_{1/2}$ of a complex, the catalytic rate is often lowered as well. Often, inverse linear relationships can be found under electrocatalytic conditions, but not exclusively. Also, there might be no clear relationship between the electronic effects of the ligand and the catalytic rate. Lastly, these electronic effects might even change the mechanism. All of these mechanistic features can only be revealed by SAR studies.

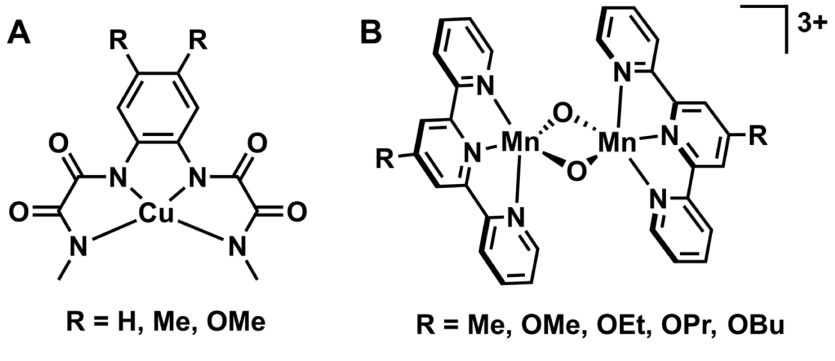

Chart 1.6. Ligands of the tetra-anionic copper complexes (A) and the terpyridine manganese complexes (B) for electrochemical water oxidation.

1.2.2 Stability of molecular complexes under electrochemical conditions

A major issue of molecular complexes is their stability under electrochemical conditions.[97-99] They can degrade by forming an electrodeposition of metallic layers or metal oxides depending on reductive or oxidative conditions. One origin for this type of degradation can be a very fast ligand exchange rate.[100] Cu^{2+} in particular has very fast exchange rates. For example, exchange rates in the order 10^7 to 10^9 s^{-1} for the exchange of the ligand in $[Cu(1,2\text{-diaminoethane})_3]^{2+}$ and $[Cu(H_2O)_6]^{2+}$ complexes have been determined, respectively. For comparison, $[Ir(H_2O)_6]^{3+}$ has an exchange rate of 1.1×10^{-10} s^{-1} at room temperature. As these reactions are equilibriums, a very low concentration of unchelated metal is present at all times, despite high binding constants of a ligand. Under reductive potentials, this could form a metallic deposit which disturbs the equilibrium with the chelated complex. For copper complexes, this equilibrium is re-established within the order of nanoseconds. As the deposited, solid metallic copper is not included in the equilibrium, the overall concentration of the chelated copper complex is lowered. Therefore, copper complexes can easily degrade by deposition in the time scale of a short cyclic voltammogram. The actual rate of deposition would be dependent on potential and the binding strength of the ligand to copper, but at low reductive potentials this is a very likely process. Apart from electrochemical conditions, this fast ligand exchange rate can also affect sacrificial reagent driven water oxidation. For copper catalysts, ligand chelation to Ce^{IV} can take place through the same route as described above thereby lowering the copper complex concentration and inhibiting reactivity from Ce^{IV}. For other complexes, such as the aforementioned iridium aqua complex, ligand exchange rate is so slow that this deposition pathway is not applicable. In those cases, other decomposition pathways are of importance. Generally, ligand oxidation by reactive (radical) intermediates is the major degradation pathway, but the formation of an inactive complex is also possible. One example is the electrochemical study that compared Cp* versus Cp iridium complexes (Cp = cyclopentadienyl). Cp complexes had a rather low activity,[101] later suggested[38] to stem from the formation of an inactive dimerized μ-oxo complex that cannot be formed when Cp* was used as ligand. As will be discussed next, the Cp* ligand can degrade itself and the remaining iridium moieties can dimerize to form μ-oxo-bridged species,[102] which is in contrast to this proposed hypothesis of deactivation of Cp iridium complexes by dimerization. Some studies report ligand degradation or even the formation of iridium oxide (IrO_x) nanoparticles during or after catalysis.[103-128] The high water oxidation activity found by studies involving the

simple $[Cp^*Ir(H_2O)_3]^{2+}$ complex initiated research into the, now well-established, breakdown routes of the Cp* ligand for various complexes.[103-119, 129] For $[Cp^*Ir(H_2O)_3]^{2+}$, this results in IrO_x electrodeposition as after Cp* degradation only iridium aqua species remain that easily deposit.[122] Also, (substituted) bipyridine Cp* complexes oxidatively degrade into inert deposits under electrochemical conditions as opposed to some structure-activity relationships observed with chemical oxidants.[117]

1.2.3 Influence of the ligand on heterogenized systems

Often, complexes are intentionally immobilized on the surface of an electrode to be able to combine the advantages of homo- and heterogeneous catalysis. Here, a distinction between two strategies has to be made. Immobilizing a complex onto the electrode surface has the goal to use the intact complex whereas some strategies merely use this complex as a pre-catalyst for a transformation to the active and heterogenized species by for example (intentional) ligand oxidation or electrodeposition. For the first strategy, many studies utilize an anchor group (thiol, pyrene linker) on the ligand that serves as a tether between the electrode surface and the complex. General methods are covalent bonding with metal oxo surfaces,[130, 131] self-assembled monolayers of thiol moieties with a gold surface,[132] electrografting of diazonium salts to carbon or metal surfaces,[133] π-π stacking based adsorption with pyrene linkers or Nafion-assisted dropcasting.[134, 135] Notably, bringing complexes in close contact with the electrode can change intrinsic properties such as the redox couples which inherently influences the catalytic activity as opposed to the homogeneous complex. An example is a trispyridyl Cu^{II} complex that was found to be more stable in the Cu^{I} state when tethered on the electrode via a thiol moiety.[136] On the other hand, adsorbed cobalt hangman corroles (Chart 1.7) still benefited from electron withdrawing substituents for water oxidation, thus structure–activity relationships can still prevail.[135]

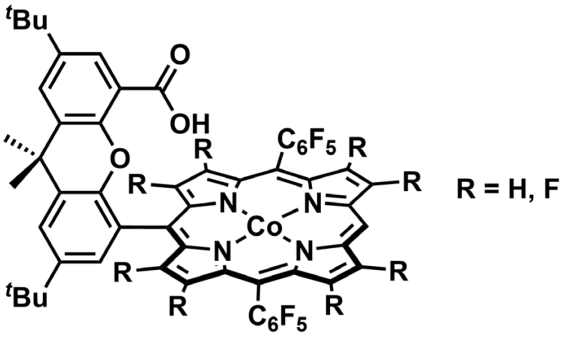

Chart 1.7. Substituted cobalt hangman corroles.

An interesting alternative to the aforementioned immobilization strategies, are pyrazine linkages between graphitic electrodes and the complex. In contrast to traditional, tether-based anchoring, this method is suggested to allow for fast electron-transfer kinetics by incorporating the catalysts as part of the electrode thereby facilitating conjugation through the pyrazine linkage (Scheme 1.2).[137]

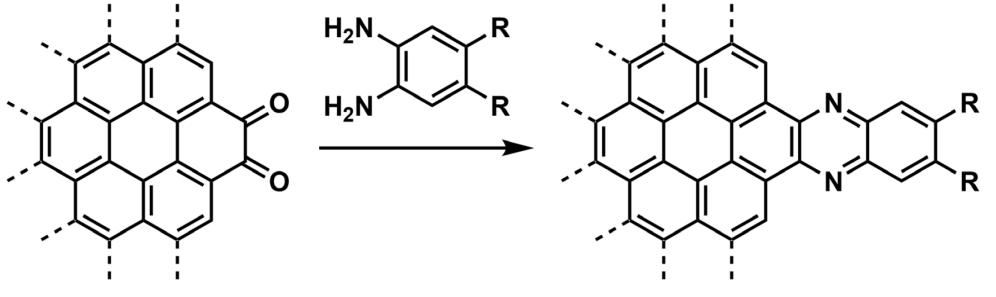

Scheme 1.2. Immobilization of catalysts through pyrazine conjugation with graphitic carbon electrodes.

The second strategy is using molecular complexes as pre-catalysts. Basically, this strategy includes an expected (as often claimed) decomposition of the parent complex (or pre-catalyst) that results in the desired catalyst. For example, after oxidation of the Cp* moiety of [Cp*Ir(pyalc)(Cl)] (pyalc = 2-(2'pyridyl)-2-propanolate)[102, 109, 115, 116, 122] the complex turns into a dinuclear species with the pyalc ligands still coordinating to the iridium cores (Scheme 1.3). This species has later been immobilized on a metal oxide and it was shown that over 90% of the iridium atoms were involved in catalysis.[102] Such an approach could be very beneficial for reducing catalyst loadings in electrolyzers.

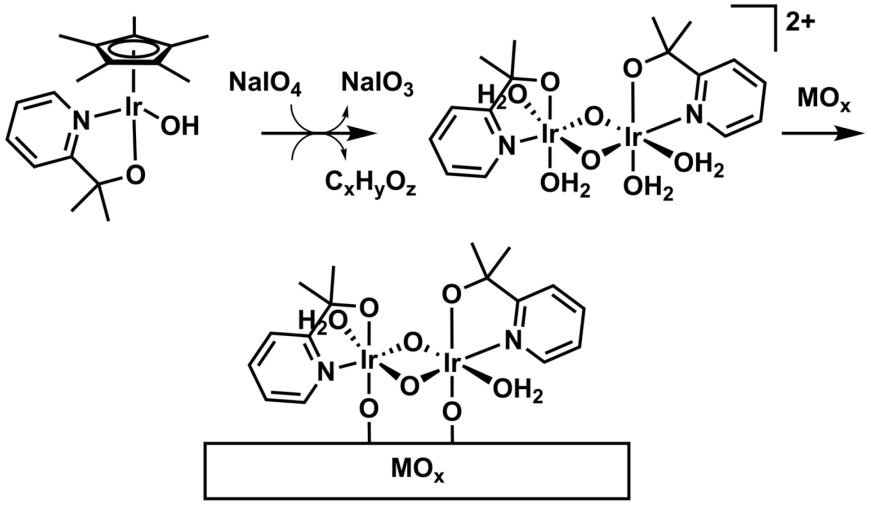

Scheme 1.3. Oxidative degradation and subsequent immobilization of the active species formed by [Cp*Ir(pyalc)(OH)].[102]

Another example shows that by picking the right potential and under the influence of the ligand a copper complex could be transformed to copper oxide with increased water oxidation activity and inhibited copper stripping at high oxidative potentials.[138] Optimizing nanoparticle sizes is another field where molecular-pre-catalysts or ligands play a role. Sometimes ligands are used to "cap" nanoparticles to control the nanoparticle size. However, ligands might actually participate in nanoparticle catalysis and thereby influencing selectivity and activity.[139, 140] Striking examples include ligand induced inhibition of undesired phosphate adsorption on the surface of platinum nanoparticles,[141] or actually improving the ORR activity of platinum nanoparticles with electron withdrawing ligands. In the study of Zhou *et al.*, a clear Hammett correlation with the ORR activity could be found emphasizing the power of the synthetic versatility of ligands (Figure 1.4).[142]

1.3 Electrochemical techniques for the analysis of molecular complexes

1.3.1 Analyzing the kinetics of the catalytic reaction

The practice of studying electrocatalysis by molecular complexes has been well described in many reviews and tutorials.[143-149] Most often, the current response when the potential is cycled with a three-electrode setup is recorded in a cyclic voltammogram (CV) that reveals redox couples and catalytic currents. In addition,

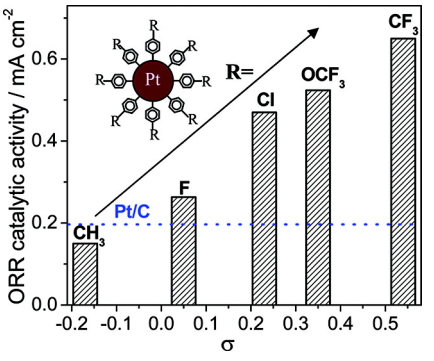

Figure 1.4. Concept of *para*-substituted phenyl groups capping Pt nanoparticles and the correlation between the Hammett parameter and the ORR activity. Adapted from Zhou *et al.*[142]

there are several other electrochemical techniques that can be used. Though a lot of information can be extracted from these techniques, the underlying theory is often based on certain assumptions. This section discusses both the application of these techniques towards the study of molecular complexes including any pitfalls that may lead to a wrong interpretation when the theoretical background is not considered completely.

Analyzing the kinetics of an electrocatalytic reaction catalyzed by a homogeneous, molecular complex is different than in traditional homogeneous catalysis with sacrificial reagents, because catalysis is only taking place near the electrode surface. Nevertheless, it is possible to establish the rate of catalysis. The current enhancement method can be used to directly determine the observed rate constant of a reaction (k_{obs}).[150] It uses the ratio between the maximum current of the catalytic wave i_{cat} and the peak current of the reduction or oxidation of the complex i_p (depending on the catalytic reaction). From this ratio, k_{obs} can be calculated according to Equation 1.4 with n being the number of electrons, R the gas constant, T the temperature (in Kelvin), F Faradays constant, and ν the scan rate (in V/s).

$$\frac{i_{cat}}{i_p} = \frac{n}{0.4463}\sqrt{\frac{RTk_{obs}}{F\nu}} \qquad \textbf{Eqn. 1.4}$$

A downside of using the current enhancement method is that the catalytic peak current is used. This current can be heavily affected by mass transport limitations resulting in cases where for example the catalyst might be intrinsically very fast, but the k_{obs} is low due to fast substrate consumption. One way to overcome

this problem, is to use the foot of the wave analysis (FOWA).[145-148] The FOWA is elaborated in Chapter 5, but in short, the FOWA allows to determine the (theoretical) maximum TOF (TOF_{max}) of the catalyst by analyzing the catalytic current close to the onset potential where it is assumed that the current is purely kinetic in nature. The downside is that precise knowledge of the mechanism is required to be able to correctly apply the FOWA. Also, the TOF_{max} is a theoretical rate which might never truly be obtained for instance due to catalyst degradation.

Another technique for studying the kinetics is to construct a Tafel plot. This plot can, in an ideal case, be used to benchmark catalysts and to get mechanistic insight. A Tafel plot is a plot of the overpotential (or potential) *versus* the logarithm of the current density (current per active surface area). In an ideal case, the linear part of the obtained plot is described by the Tafel equation (Equation 1.5 in a simple form).[151] The major assumption, and pitfall when used incorrectly, is that the Tafel equation is only valid for a situation where the concentration of the substrate near the electrode is equal to the bulk concentration. In other words, the mass transport rate should be far larger than the kinetic rate. The current used for the Tafel plot should be the kinetic current I_k, which may be derived by using Equation 1.6 (see next section). In a heterogeneous system, the Tafel slope (A, V/dec) can be used to compare catalytic behavior. With a lower the magnitude of the slope, more catalytic current will be generated when the overpotential is increased which is characteristic for a better catalyst. i_o is the exchange current density, which is the intersection with the x-axis when the linear part of a Tafel plot is extrapolated. In simple terms, this current is the theoretical current at 0 V potential. The higher this number, the better the catalyst. Even for heterogeneous catalysts, ideal conditions may not be met when the current is not a 100% Faradaic current for the reaction of interest. Instead, catalyst decomposition or unwanted side reactions can contribute to the overall current as well. For homogeneous systems, the applicability might be limited since the diffusion of the catalyst itself plays a role. The theoretical background of the Tafel equation assumes that the catalyst is a heterogeneous and stationary surface. Nevertheless, Tafel plots might still be useful for catalyst benchmarking or mechanistic insight. The next section gives an example the use of the rotating ring disk electrode (RRDE) setup in combination with a Tafel analysis.

$$\eta = A \times \log\left(\frac{i}{i_0}\right) \qquad \textbf{Eqn. 1.5}$$

Another technique that can be used is (chrono)amperometry in which the applied potential is fixed and the current monitored over time. This would reveal any activation/deactivation processes but it also allows for bulk electrolysis (also called controlled potential electrolysis). The latter technique affects the entire bulk solution by employing large surface area electrodes, stirring of the solution, and separating the counter and work electrodes. This way, one might be able to replicate sacrificial reagent conditions where the bulk of the solution is utilized as well and TON/TOF calculations might be made. In addition, post-catalytic spectroscopic studies of the bulk solution become possible. These studies can help to detect intermediates/products and any degraded catalyst. Of note, it is impossible to accurately determine after what period of time bulk electrolysis has affected the entire solution which can lead to wrong interpretations. If one performs bulk electrolysis to check whether the catalyst remains intact, the post-catalytic spectroscopic observation of intact catalyst does not necessarily indicate that the catalyst is stable nor could any ratio of degraded *versus* intact complex be determined. Instead, it might be that this portion of intact catalyst has never been in contact with the electrode during the duration of the experiment. Nevertheless, bulk electrolysis can allow for the qualitative detection of any intermediate, product, or degraded complex in combination with other techniques that are discussed in the next section.

1.3.2 Determining the product distribution

One of the most powerful electrochemical techniques to study the product distribution of a catalytic reaction is the RRDE setup. This electrochemical setup allows for control over the diffusion of electrolyte towards the electrode. By rotating a disk electrode, a laminar flow of electrolyte towards the surface of that electrode is established (Figure 1.5). That way, the obtained current is no longer dependent on time and thus on the scan rate (as would be predict by for instance the Randles-Sevcik equation, see next section) but purely on the electrode rotation speed as variable. In addition, a ring electrode could be used around the disk to detect products that are formed on the disk and thus the product selectivity could be derived. Most often, this ring electrode is a Pt electrode. In O_2 reduction, H_2O_2 can be detected by setting a ring potential of 1.2 V where H_2O_2 is oxidized to O_2, but H_2O is not oxidized. Central to its usage is the collection efficiency (N_{coll}). Not 100% of the products formed at the disk will be detected at the ring due to geometrical constraints. Therefore, a well-defined redox couple such as the $[Fe(CN)_6]^{4-}/[Fe(CN)_6]^{3-}$ redox couple is often used to determine the ring to disk

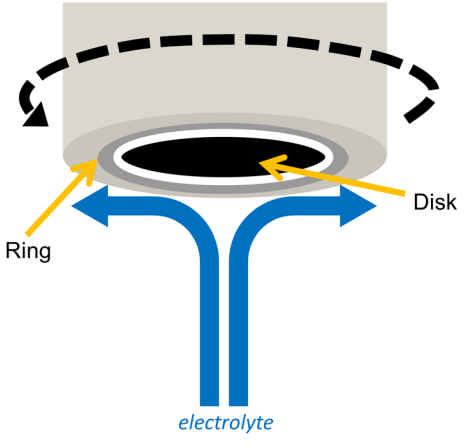

Figure 1.5. Schematic representation of a rotating ring disk electrode.

ratio which is N_{coll} in that case (Figure 1.6). Importantly, Pt is not always the best ring electrode as, for example, H_2O_2 oxidation was found to be not mass transport limited under alkaline conditions.[152] Instead, Au was suggested as better a better option for the ring electrode under those conditions. As discussed in Appendix C of this thesis, the Pt ring is also not a steady sensor for H_2O_2 at pH 7 in phosphate buffer, especially for longer measurements (hours). The N_{coll} can become less during the measurement due to, for instance, PtO_x formation. Also, the polish method of the electrode plays a role and the N_{coll} may vary after each polish. A good practice would be to determine the N_{coll} before each catalytic experiment preferably with the substrate of interest, instead of the $[Fe(CN)_6]^{4-}/[Fe(CN)_6]^{3-}$ redox couple. For longer experiments, such as bulk electrolysis, the RRDE setup is less reliable for quantitative assessment of the product distribution and the RRDE measurement could be complemented with other techniques to determine the product ratio such as gas chromatography, mass spectrometry, or by titration of the formed products such as the titration of H_2O_2 with $KMnO_4$.

The current that is obtained with the disk electrode, where catalysis takes place, is generally described by Equations 1.6 and 1.7 which are the Koutecký-Levich and Levich equations, respectively.[151] In an ideal case, the contributions of the kinetic current I_k (in absence of mass transport limitations) and diffusion limited current I_L are described by Equation 1.6. The diffusion limited current is the maximum current that can be obtained at a certain rotation rate ω (in rad/s) and is only dependent on physical constants. Apart from earlier mentioned physical constants, the current is

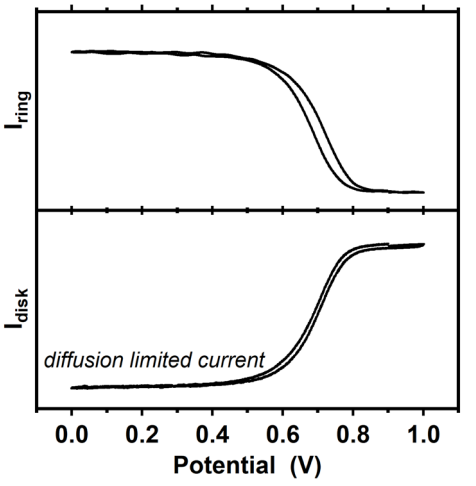

Figure 1.6. Typical RRDE response of the reduction of $[Fe(CN)_6]^{3-}$ to $[Fe(CN)_6]^{4-}$ on the disk (bottom panel) and the re-oxidation to $[Fe(CN)_6]^{3-}$ on the ring (top panel).

also dependent on ν_k which is the kinematic viscosity of the electrolyte in cm^2/s, the electrode surface area A (in cm^2), the bulk concentration of the complex C_0 (in mol/cm^3), the diffusion coefficient of the complex D_0 (in cm^2/s).

$$\frac{1}{I} = \frac{1}{I_k} + \frac{1}{I_L} \qquad \textbf{Eqn. 1.6}$$

$$I_L = 0.62nFAD_O^{2/3}C_O\nu_k^{-1/6}\omega^{1/2} \qquad \textbf{Eqn. 1.7}$$

These equations have many uses, but an important use is to determine n: the number of electrons transferred in the reaction. This number can give information about the product selectivity of the reaction. For example, an electron transfer number of 2 would indicate that H_2O_2 is the major product for O_2 reduction whereas a number of 4 would point towards H_2O as product. Any number in between will tell something about the selectivity. When performing RRDE in the potential window of I_L, n can be determined by varying the rotation rate. Important to realize is that these equations have been developed for single-step, one-way reactions. In reality, most catalysis is not. For example, a study by Qiao and co-workers in alkaline electrolyte showed that n for the O_2 reduction reaction depended on the rotation rate ω which opposes Equation 1.7 that states it should remain constant.[152] Another key aspect is that homogeneous catalysts are freely diffusive species as well. Equations 1.6 and 1.7 are tailored for a heterogeneous electrocatalysts that are, or situated on, the disk

electrode. If the catalytic rate (TOF) of a homogeneous complex is not fast enough, the catalyst might not complete a full catalytic cycle before it has passed the electrode surface and is thus interrupted. Very slow rotation could help, but in that case steady state conditions will only be achieved at very low scan rates[151] and considerable lag between the disk and ring current response is observed.[153] The exact limit of the TOF is not known, since it would depend on, among others, the diffusion coefficient and whether or not the complex can adsorb on the electrode. In that sense, even fast catalysts could even be affected.

The kinetic current I_k that can be obtained by Equation 1.6 can be used for the construction of a Tafel plot, as described in the previous section. As said, the Tafel analysis can be used to benchmark catalysts and for mechanistic studies. For example, a Tafel analysis was performed for the electrochemical O_2 and H_2O_2 reduction by a copper trispyridyl complex.[154] In this study, the Tafel plot for O_2 reduction had two linear regions with different Tafel slopes. One of the slopes corresponded to the slope of the linear region of the Tafel plot for H_2O_2 reduction. This finding, combined with observation of H_2O_2 on the ring electrode in specific potential windows, led to the conclusion that O_2 was reduced in a stepwise 2+2 reduction with H_2O_2 as intermediate and thus that O_2 was reduced by two, consecutive catalytic cycles.

1.3.3 Techniques to determine the homogeneity of the active species

Several techniques can be employed to determine whether degradation of the molecular complex has taken place, which new species are formed and whether they are the active catalyst. The simple rinse-test is the most often mentioned control experiment showing that no deposit has formed on the electrode. In this test, the electrode is rinsed after being in contact with the catalyst (and optionally having performed electrocatalysis) and subsequently tested in catalyst-free electrolyte. This test will give a first indication whether a deposit is formed and if it is catalytically active. Mistakenly, this test is often the sole evidence for the presence or absence of any deposit (and thus catalyst degradation). This would either ignore cases with catalytically inactive deposits or deposits that reversibly desorb as soon the potential is lifted.[155-157] Moreover, discrepancies between the before and after voltammograms could be incorrectly be assigned to catalyst degradation. The latter case is especially important in the case of glassy carbon. This electrode is widely employed for studying homogeneous complexes. However, electrode corrosion can alter its voltametric response even in the absence of catalyst. At high potential and depending on pH, glassy carbon can severely degrade and as a result increase the double layer

capacitance and significantly affect the CV or amperogram (see also Chapter 2 and Appendix A).[158] In general, electrodes are not inert substances and, depending on conditions, can actually degrade during the experiment.[159] Therefore, a rinse test should always be complemented with other techniques to establish whether catalyst degradation and/or deposition takes place.

Another often used simple technique is to record CV's at different scan rates and plot the peak current of the redox couples against the scan rate or the square root of the scan rate. The idea behind this technique is that homogeneous species will give a linear relationship with the square root of the scan rate, which is based on the Randles-Sevcik equation (Equation 1.8).[151] The equation describes the relationship between the scan rate at which the potential is swept ν (in V/s) and the peak current i_p (in A) of a redox reaction. Important to note, is that this equation considers the peak current of a redox process in which diffusion plays a role. In this case, there is a diffusion layer between unaffected species in the bulk of the electrolyte and electrochemically converted species near the electrode surface. The size of diffusion layer determines how quickly unreacted species can diffuse to the electrode and subsequently converted. The size of this layer is dependent on the scan rate: a faster scan rate yields a smaller diffusion layer. As a consequence, at a higher scan rate more unreacted species can diffuse to the electrode and thus the peak current of the reduction or oxidation is larger.[143] The Randles-Sevcik equation can be put to use in several ways to investigate molecular complexes. First of all, the diffusion coefficient of a diffusive species can be calculated when the electron transfer number is known. In addition, if the reduction/oxidation of the complex corresponds to diffusive process, the peak current of that redox reaction is proportional to $\nu^{1/2}$. If diffusion does not play a role, the peak current is directly proportional to ν.[151] Usually, the diffusive species is the homogeneous complex. This equation is therefore often used to prove that a species is homogeneous. However, finding that a redox couple is related to a diffusive process does not necessarily prove this. For example, complexes that have been tethered on the surface of electrodes can also be regarded as diffusive species when they have freedom of movement due to flexible tethers and will give a peak current *versus* $\nu^{1/2}$ relationship. As a consequence, one could wrongly conclude that heterogenization by ligand tethering has failed.

$$i_p = 0.4463nFAC_0\left(\frac{nF\nu D_0}{RT}\right)^{\frac{1}{2}} \qquad \textbf{Eqn. 1.8}$$

A direct method to study deposition *in operando* is the electrochemical quartz crystal microbalance (EQCM). This technique can monitor the weight changes of the electrode during the measurement. In the ideal case, features of the cyclic voltammogram can be directly linked to electrodeposition, deposit stripping, or the absence of these phenomena and thus direct evidence for the homogeneity of a molecular complex under electrochemical conditions.[86, 122, 128, 138, 160] This technique is based on the vibration of a quartz crystal on which the electrode surface resides. Key to EQCM is the Sauerbrey equation (Equation 1.9).[161]

$$\Delta f = -\frac{2{f_0}^2}{A\sqrt{\rho_q \mu_q}}\Delta m \qquad \textbf{Eqn. 1.9}$$

Here, the frequency change Δf of the quartz crystal is measured and can be linked to the mass change of the electrode Δm (g/cm^2) by the surface area of the crystal (A, cm^2), the nominal frequency resonant frequency of the crystal (f_0, 6 MHz for the setup used), the density of quartz (ρ_q, g/cm^3), and the shear modulus of quartz (μ_q, g/cm s^2). In practice, $\frac{2{f_0}^2}{A\sqrt{\rho_q \mu_q}}$ can be replaced by a sensitivity coefficient that can be experimentally determined with a known electrochemical deposition process such as Pb deposition.[128, 162] Of note, a relative negative frequency change with respect to the pre-experimental oscillation frequency corresponds to a mass increase.

Importantly, Equation 1.9 was originally derived for crystals that are in contact with air. For liquid interfaces, the density and viscosity of the liquid affect the oscillation frequency.[163] Under catalytic conditions, where substrates are consumed at a fast pace and possibly gaseous products are formed, the frequency can change without any actual deposit forming or stripping by, for example, changes in hydrophobicity of the electrode surface or the viscosity of the electrolyte.[164] Moreover, small frequency changes can relate to catalyst adsorption/desorption rather than electrodeposition and catalyst degradation. For these reasons, results of EQCM data are best combined with *ex-situ* spectroscopic surface studies. Several spectroscopic techniques are available that can detect the size of the deposit (tunneling or scanning electron microscopy), soluble colloidal particles (dynamic light scattering), and the elemental composition of the electrode surface (various X-ray techniques such as X-ray photoelectron microscopy, energy-dispersive X-ray spectrometry, X-ray absorption spectroscopy).[97-99] These techniques complement

each other and provide a powerful tool as is demonstrated in Chapters 2 and 3. EQCM is a quick technique for a first *in operando* check of electrodeposition and more informative than the above-mentioned simple rinse test and scan rate dependence studies. Determination of the homogeneity and the nature of the active species is very important to avoid incorrect conclusions and these studies should be done with several techniques instead of relying on just one.

1.4 Scope of thesis

The brief review of molecular catalysts in electrocatalysis shows that structure–activity relationships can be found within electrocatalysis by molecular complexes. On the other hand, decomposition of these molecular catalysts is a significant issue in electrocatalytic studies and should always be kept in mind when studying new catalysts. Chapters 2 and 3 discuss such electrochemical decomposition studies for several iridium complexes for water oxidation and a copper based oxygen reduction catalyst, respectively. Chapters 4 and 5 discuss molecular copper complexes for which the active species is the complex itself. Here, structural adjustments such as linking active sites (Chapter 4) and placing electron withdrawing substituents (Chapter 5) are shown to directly affect catalytic rates and selectivity.

In Chapter 2, the electrochemical study of several known molecular iridium complexes for OER is elaborated. Structure–activity relationships that were previously obtained under sacrificial reagent conditions did not prevail. By using a combination of spectroscopic techniques such as XPS, UV-vis and NMR, and electrochemical techniques such as EQCM we have been able to show that these complexes suffer from ligand oxidation, such as Cp* degradation, and form catalytically active deposits on the electrode. Nevertheless, small, ligand-induced differences in activity were observed and, combined with XPS characterization, led to the suggestion that small IrO_x clusters with incorporated ligand residues were responsible for the catalytic activity.

In Chapter 3, it is shown that a triazole based copper complex, previously regarded as the benchmark for O_2 reduction for molecular copper complexes, disintegrates to form a metallic copper layer under electrochemical conditions. This result was obtained by simply mixing the salt and ligand with a carbon support (the previously reported procedure), as well as for an *in situ* generated complex. Again, a combination of spectroscopic techniques (EPR, SQUID, UV-vis, XPS) and EQCM was employed to identify the copper deposition as the active species. In addition, we

were able to show that the triazole ligand still influences the deposit as it prevents this metallic layer from being oxidatively stripped close to the onset of O_2 reduction.

In Chapter 4, a molecular copper complex, consisting of two fused mononuclear copper complexes through a covalent bond, is reported to drastically change the O_2 reduction selectivity to H_2O_2 instead of H_2O. Furthermore, high Faradaic efficiencies for the formation of H_2O_2 were obtained over prolonged measurements. For the first time, elaborate bulk electrolysis experiments for H_2O_2 production with a molecular complex have been performed for which factors that negatively affect catalyst stability were identified. The experimental design was optimized by, for instance, applying Cu^0 stripping intervals, to directly improve the Faradaic efficiency.

In the last experimental chapter, Chapter 5, substituted copper trispyridyl complexes are discussed. The effect of electron donating or withdrawing substituents on the electrochemical O_2 and H_2O_2 reduction was investigated. Remarkably, the onset potential of O_2 reduction was not affected leading to a new insight into the observed O_2 to H_2O_2 reduction mechanism that was taking place on the time scale of the experiment. On the other hand, we found that electron withdrawing substituents substantially improved both the onset potential and rate for H_2O_2 reduction.

Overall, this thesis focusses on ligand effects in electrocatalysis by molecular (pre)catalysts and proper characterization of the active species. In all cases, the ligand plays a role in catalytic activity of the complex, its decomposition, and/or in the catalytic activity of the deposited active species.

1.5 References

1. IPCC, *Climate Change 2013: The Physical Science Basis. Contribution of Working Group I to the Fifth Assessment Report of the Intergovernmental Panel on Climate Change*. Cambridge University Press: Cambridge, United Kingdom and New York, NY, USA, 2013; p 1535.
2. Cano, Z. P.; Banham, D.; Ye, S.; Hintennach, A.; Lu, J.; Fowler, M.; Chen, Z., *Nat. Energy* **2018,** *3*, 279–289.
3. Paets van Troostwyk, A.; Deiman, J. R., *Obser phys hist na* **1789,** *35*, 369–378.
4. Bratsch, S. G., *J. Phys. Chem. Ref. Data* **1989,** *18*, 1–21.
5. Dau, H.; Limberg, C.; Reier, T.; Risch, M.; Roggan, S.; Strasser, P., *ChemCatChem* **2010,** *2*, 724–761.
6. Carmo, M.; Fritz, D. L.; Mergel, J.; Stolten, D., *Int. J. Hydrogen Energy* **2013,** *38*, 4901–4934.
7. Hans Wedepohl, K., *Geochim. Cosmochim. Acta* **1995,** *59*, 1217–1232.
8. Parry, S. J., *Chem. Geol.* **1984,** *43*, 115–125.
9. Gasteiger, H. A.; Kocha, S. S.; Sompalli, B.; Wagner, F. T., *Appl. Catal., B* **2005,** *56*, 9–35.
10. Gewirth, A. A.; Thorum, M. S., *Inorg. Chem.* **2010,** *49*, 3557–3566.
11. Koper, M. T. M., Catalysis of Redox Reactions. In *Comprehensive Inorganic Chemistry II (Second Edition)*, Reedijk, J.; Poeppelmeier, K., Eds. Elsevier: Amsterdam, 2013; Vol. 8, pp 459–474.
12. Abild-Pedersen, F.; Greeley, J.; Studt, F.; Rossmeisl, J.; Munter, T. R.; Moses, P. G.; Skúlason, E.; Bligaard, T.; Nørskov, J. K., *Phys. Rev. Lett.* **2007,** *99*, 016105.
13. Orfanidi, A.; Madkikar, P.; El-Sayed, H. A.; Harzer, G. S.; Kratky, T.; Gasteiger, H. A., *J. Electrochem. Soc.* **2017,** *164*, F418–F426.

14. Gröger, O.; Gasteiger, H. A.; Suchsland, J.-P., *J. Electrochem. Soc.* **2015,** *162*, A2605–A2622.
15. Kongkanand, A.; Mathias, M. F., *J. Phys. Chem. Lett.* **2016,** *7*, 1127–1137.
16. Goor, G., *Catalytic Oxidations with Hydrogen Peroxide as Oxidant*. Kluwer Academic Publishers: The Netherlands, 1992.
17. Legrini, O.; Oliveros, E.; Braun, A. M., *Chem. Rev.* **1993,** *93*, 671–698.
18. Metcalf & Eddy Inc.; Tchobangolous, G., *Wastewater Engineering: Treatment and Resource Recovery*. 5th edition ed.; Mcgraw-Hill Education: 2014.
19. Hage, R.; Lienke, A., *Angew. Chem. Int. Ed.* **2006,** *45*, 206–222.
20. Süss, H. U., Bleaching. In *Ullmann's Encyclopedia of Industrial Chemistry*, 2012.
21. Campos-Martin, J. M.; Blanco-Brieva, G.; Fierro, J. L. G., *Angew. Chem. Int. Ed.* **2006,** *45*, 6962–6984.
22. Eul, W.; Moeller, A.; Steiner, N., Hydrogen Peroxide. In *Kirk-Othmer Encyclopedia of Chemical Technology* [Online] John Wiley & Sons, Inc.: 2000. http://dx.doi.org/10.1002/0471238961.0825041808051919.a01.pub2.
23. Siahrostami, S.; Verdaguer-Casadevall, A.; Karamad, M.; Deiana, D.; Malacrida, P.; Wickman, B.; Escudero-Escribano, M.; Paoli, E. A.; Frydendal, R.; Hansen, T. W.; Chorkendorff, I.; Stephens, I. E. L.; Rossmeisl, J., *Nat. Mater.* **2013,** *12*, 1137–1143.
24. Verdaguer-Casadevall, A.; Deiana, D.; Karamad, M.; Siahrostami, S.; Malacrida, P.; Hansen, T. W.; Rossmeisl, J.; Chorkendorff, I.; Stephens, I. E. L., *Nano Lett.* **2014,** *14*, 1603–1608.
25. Jirkovský, J. S.; Panas, I.; Ahlberg, E.; Halasa, M.; Romani, S.; Schiffrin, D. J., *J. Am. Chem. Soc.* **2011,** *133*, 19432–19441.
26. Jiang, Y.; Ni, P.; Chen, C.; Lu, Y.; Yang, P.; Kong, B.; Fisher, A.; Wang, X., *Adv. Energy Mater.* **2018,** *8*, 1801909.
27. Song, C.; Zhang, J., Electrocatalytic Oxygen Reduction Reaction. In *PEM Fuel Cell Electrocatalysts and Catalyst Layers: Fundamentals and Applications*, Zhang, J., Ed. Springer London: London, 2008; pp 89–134.
28. Chen, S.; Chen, Z.; Siahrostami, S.; Kim, T. R.; Nordlund, D.; Sokaras, D.; Nowak, S.; To, J. W. F.; Higgins, D.; Sinclair, R.; Nørskov, J. K.; Jaramillo, T. F.; Bao, Z., *ACS Sustainable Chem. Eng.* **2018,** *6*, 311–317.
29. Liu, Y.; Quan, X.; Fan, X.; Wang, H.; Chen, S., *Angew. Chem. Int. Ed.* **2015,** *54*, 6837–6841.
30. Kim, H. W.; Ross, M. B.; Kornienko, N.; Zhang, L.; Guo, J.; Yang, P.; McCloskey, B. D., *Nat. Catal.* **2018,** *1*, 282–290.
31. Lu, Z.; Chen, G.; Siahrostami, S.; Chen, Z.; Liu, K.; Xie, J.; Liao, L.; Wu, T.; Lin, D.; Liu, Y.; Jaramillo, T. F.; Nørskov, J. K.; Cui, Y., *Nat. Catal.* **2018,** *1*, 156–162.
32. Iglesias, D.; Giuliani, A.; Melchionna, M.; Marchesan, S.; Criado, A.; Nasi, L.; Bevilacqua, M.; Tavagnacco, C.; Vizza, F.; Prato, M.; Fornasiero, P., *Chem* **2018,** *4*, 106–123.
33. Chen, S.; Chen, Z.; Siahrostami, S.; Higgins, D.; Nordlund, D.; Sokaras, D.; Kim, T. R.; Liu, Y.; Yan, X.; Nilsson, E.; Sinclair, R.; Nørskov, J. K.; Jaramillo, T. F.; Bao, Z., *J. Am. Chem. Soc.* **2018,** *140*, 7851–7859.
34. Han, L.; Sun, Y.; Li, S.; Cheng, C.; Halbig, C. E.; Feicht, P.; Hübner, J. L.; Strasser, P.; Eigler, S., *ACS Catal.* **2019,** *9*, 1283–1288.
35. Fellinger, T.-P.; Hasché, F.; Strasser, P.; Antonietti, M., *J. Am. Chem. Soc.* **2012,** *134*, 4072–4075.
36. Costentin, C.; Dridi, H.; Savéant, J.-M., *J. Am. Chem. Soc.* **2015,** *137*, 13535–13544.
37. Chan, R. J. H.; Su, Y. O.; Kuwana, T., *Inorg. Chem.* **1985,** *24*, 3777–3784.
38. Blakemore, J. D.; Crabtree, R. H.; Brudvig, G. W., *Chem. Rev.* **2015,** *115*, 12974–13005.
39. Singh, A.; Spiccia, L., *Coord. Chem. Rev.* **2013,** *257*, 2607–2622.
40. Limburg, B.; Bouwman, E.; Bonnet, S., *Coord. Chem. Rev.* **2012,** *256*, 1451–1467.
41. Pegis, M. L.; Wise, C. F.; Martin, D. J.; Mayer, J. M., *Chem. Rev.* **2018,** *118*, 2340–2391.
42. Anand, M.; Nørskov, J. K., *ACS Catal.* **2020,** *10*, 336–345.
43. Solomon, E. I.; Sundaram, U. M.; Machonkin, T. E., *Chem. Rev.* **1996,** *96*, 2563–2606.
44. Soukharev, V.; Mano, N.; Heller, A., *J. Am. Chem. Soc.* **2004,** *126*, 8368–8369.
45. Mano, N.; Soukharev, V.; Heller, A., *J. Phys. Chem. B* **2006,** *110*, 11180–11187.
46. Blanford, C. F.; Heath, R. S.; Armstrong, F. A., *Chem. Commun.* **2007**, 1710–1712.
47. Pita, M.; Mate, D. M.; Gonzalez-Perez, D.; Shleev, S.; Fernandez, V. M.; Alcalde, M.; De Lacey, A. L., *J. Am. Chem. Soc.* **2014,** *136*, 5892–5895.
48. Thorum, M. S.; Anderson, C. A.; Hatch, J. J.; Campbell, A. S.; Marshall, N. M.; Zimmerman, S. C.; Lu, Y.; Gewirth, A. A., *J. Phys. Chem. Lett.* **2010,** *1*, 2251–2254.
49. Cracknell, J. A.; Vincent, K. A.; Armstrong, F. A., *Chem. Rev.* **2008,** *108*, 2439–2461.
50. Calabrese Barton, S.; Gallaway, J.; Atanassov, P., *Chem. Rev.* **2004,** *104*, 4867–4886.
51. Davis, F.; Higson, S. P. J., *Biosens. Bioelectron.* **2007,** *22*, 1224–1235.

52. Solomon, E. I.; Augustine, A. J.; Yoon, J., *Dalton Trans.* **2008**, 3921–32.
53. Wasak, A.; Drozd, R.; Jankowiak, D.; Rakoczy, R., *Scientific Reports* **2019,** *9*, 3707.
54. Bullen, R. A.; Arnot, T. C.; Lakeman, J. B.; Walsh, F. C., *Biosens. Bioelectron.* **2006,** *21*, 2015–2045.
55. Thorseth, M. A.; Tornow, C. E.; Tse, E. C. M.; Gewirth, A. A., *Coord. Chem. Rev.* **2013,** *257*, 130–139.
56. Rulíšek, L.; Ryde, U., *Coord. Chem. Rev.* **2013,** *257*, 445–458.
57. Mirica, L. M.; Ottenwaelder, X.; Stack, T. D. P., *Chem. Rev.* **2004,** *104*, 1013–1046.
58. Lewis, E. A.; Tolman, W. B., *Chem. Rev.* **2004,** *104*, 1047–1076.
59. Haack, P.; Limberg, C., *Angew. Chem. Int. Ed.* **2014,** *53*, 4282–4293.
60. Serrano-Plana, J.; Garcia-Bosch, I.; Company, A.; Costas, M., *Acc. Chem. Res.* **2015,** *48*, 2397–2406.
61. Hong, S.; Lee, Y.-M.; Ray, K.; Nam, W., *Coord. Chem. Rev.* **2017,** *334*, 25–42.
62. Solomon, E. I.; Ginsbach, J. W.; Heppner, D. E.; Kieber-Emmons, M. T.; Kjaergaard, C. H.; Smeets, P. J.; Tian, L.; Woertink, J. S., *Faraday Discuss.* **2011,** *148*, 11–39.
63. Suga, M.; Akita, F.; Hirata, K.; Ueno, G.; Murakami, H.; Nakajima, Y.; Shimizu, T.; Yamashita, K.; Yamamoto, M.; Ago, H.; Shen, J.-R., *Nature* **2015,** *517*, 99–103.
64. Limburg, J.; Vrettos, J. S.; Liable-Sands, L. M.; Rheingold, A. L.; Crabtree, R. H.; Brudvig, G. W., *Science* **1999,** *283*, 1524–1527.
65. Collomb, M.-N.; Deronzier, A., *Eur. J. Inorg. Chem.* **2009,** *2009*, 2025–2046.
66. Baffert, C.; Romain, S.; Richardot, A.; Leprêtre, J.-C.; Lefebvre, B.; Deronzier, A.; Collomb, M.-N., *J. Am. Chem. Soc.* **2005,** *127*, 13694–13704.
67. Brimblecombe, R.; Bond, A. M.; Dismukes, G. C.; Swiegers, G. F.; Spiccia, L., *Phys. Chem. Chem. Phys.* **2009,** *11*, 6441–6449.
68. Parent, A. R.; Crabtree, R. H.; Brudvig, G. W., *Chem. Soc. Rev.* **2013,** *42*, 2247–2252.
69. Gersten, S. W.; Samuels, G. J.; Meyer, T. J., *J. Am. Chem. Soc.* **1982,** *104*, 4029–4030.
70. Koelewijn, J. M.; Lutz, M.; Dzik, W. I.; Detz, R. J.; Reek, J. N. H., *ACS Catal.* **2016,** *6*, 3418–3427.
71. Gagliardi, C. J.; Vannucci, A. K.; Concepcion, J. J.; Chen, Z.; Meyer, T. J., *Energy Environ. Sci.* **2012,** *5*, 7704–7717.
72. Huynh, M. H. V.; Meyer, T. J., *Chem. Rev.* **2007,** *107*, 5004–5064.
73. Geselowitz, D.; Meyer, T. J., *Inorg. Chem.* **1990,** *29*, 3894–3896.
74. Shaffer, D. W.; Xie, Y.; Concepcion, J. J., *Chem. Soc. Rev.* **2017,** *46*, 6170–6193.
75. Duan, L.; Bozoglian, F.; Mandal, S.; Stewart, B.; Privalov, T.; Llobet, A.; Sun, L., *Nature Chem.* **2012,** *4*, 418–423.
76. Zhang, B.; Sun, L., *Chem. Soc. Rev.* **2019,** *48*, 2216–2264.
77. Duan, L.; Araujo, C. M.; Ahlquist, M. S. G.; Sun, L., *Proc. Natl. Acad. Sci.* **2012,** *109*, 15584–15588.
78. Duan, L.; Wang, L.; Inge, A. K.; Fischer, A.; Zou, X.; Sun, L., *Inorg. Chem.* **2013,** *52*, 7844–7852.
79. Wasylenko, D. J.; Ganesamoorthy, C.; Koivisto, B. D.; Henderson, M. A.; Berlinguette, C. P., *Inorg. Chem.* **2010,** *49*, 2202–2209.
80. Marelius, D. C.; Bhagan, S.; Charboneau, D. J.; Schroeder, K. M.; Kamdar, J. M.; McGettigan, A. R.; Freeman, B. J.; Moore, C. E.; Rheingold, A. L.; Cooksy, A. L.; Smith, D. K.; Paul, J. J.; Papish, E. T.; Grotjahn, D. B., *Eur. J. Inorg. Chem.* **2014,** *2014*, 676–689.
81. Codolà, Z.; Gómez, L.; Kleespies, S. T.; Que Jr, L.; Costas, M.; Lloret-Fillol, J., *Nat. Commun.* **2015,** *6*, 5865.
82. Wasylenko, D. J.; Ganesamoorthy, C.; Henderson, M. A.; Berlinguette, C. P., *Inorg. Chem.* **2011,** *50*, 3662–3672.
83. Pecht, I.; Luz, Z., *J. Am. Chem. Soc.* **1965,** *87*, 4068–4072.
84. Olivares, M.; van der Ham, C. J. M.; Mdluli, V.; Schmidtendorf, M.; Müller-Bunz, H.; Verhoeven, T. W. G. M.; Li, M.; Niemantsverdriet, J. W.; Hetterscheid, D. G. H.; Bernhard, S.; Albrecht, M., *Eur. J. Inorg. Chem.* **2020,** *2020*, 801–812.
85. Menendez Rodriguez, G.; Bucci, A.; Hutchinson, R.; Bellachioma, G.; Zuccaccia, C.; Giovagnoli, S.; Idriss, H.; Macchioni, A., *ACS Energy Lett.* **2017,** *2*, 105–110.
86. van Dijk, B.; Rodriguez, G. M.; Wu, L.; Hofmann, J. P.; Macchioni, A.; Hetterscheid, D. G. H., *ACS Catal.* **2020,** *10*, 4398–4410.
87. Hammett, L. P., *J. Am. Chem. Soc.* **1937,** *59*, 96–103.
88. Hansch, C.; Leo, A.; Taft, R. W., *Chem. Rev.* **1991,** *91*, 165–195.
89. Asahi, M.; Yamazaki, S.-i.; Itoh, S.; Ioroi, T., *Dalton Trans.* **2014,** *43*, 10705–10709.
90. Thorseth, M. A.; Letko, C. S.; Tse, E. C. M.; Rauchfuss, T. B.; Gewirth, A. A., *Inorg. Chem.* **2013,** *52*, 628–634.

91. Zhang, J.; Anson, F. C., *Electrochim. Acta* **1993,** *38*, 2423–2429.
92. McCrory, C. C. L.; Ottenwaelder, X.; Stack, T. D. P.; Chidsey, C. E. D., *J. Phys. Chem. A* **2007,** *111*, 12641–12650.
93. D'Souza, F.; Deviprasad, R. G.; Hsieh, Y.-Y., *J. Electroanal. Chem.* **1996,** *411*, 167–171.
94. D'Souza, F.; Hsieh, Y.-Y.; Deviprasad, G. R., *J. Electroanal. Chem.* **1997,** *426*, 17–21.
95. Garrido-Barros, P.; Funes-Ardoiz, I.; Drouet, S.; Benet-Buchholz, J.; Maseras, F.; Llobet, A., *J. Am. Chem. Soc.* **2015,** *137*, 6758–6761.
96. Yamazaki, H.; Igarashi, S.; Nagata, T.; Yagi, M., *Inorg. Chem.* **2012,** *51*, 1530–1539.
97. Crabtree, R. H., *Chem. Rev.* **2015,** *115*, 127–150.
98. Artero, V.; Fontecave, M., *Chem. Soc. Rev.* **2013,** *42*, 2338–2356.
99. Crabtree, R. H., *Chem. Rev.* **2012,** *112*, 1536–1554.
100. Helm, L.; Merbach, A. E., *Chem. Rev.* **2005,** *105*, 1923–1960.
101. Blakemore, J. D.; Schley, N. D.; Balcells, D.; Hull, J. F.; Olack, G. W.; Incarvito, C. D.; Eisenstein, O.; Brudvig, G. W.; Crabtree, R. H., *J. Am. Chem. Soc.* **2010,** *132*, 16017–16029.
102. Sheehan, S. W.; Thomsen, J. M.; Hintermair, U.; Crabtree, R. H.; Brudvig, G. W.; Schmuttenmaer, C. A., *Nat. Commun.* **2015,** *6*, 6469.
103. Blakemore, J. D.; Schley, N. D.; Olack, G. W.; Incarvito, C. D.; Brudvig, G. W.; Crabtree, R. H., *Chem. Sci.* **2011,** *2*, 94–98.
104. Savini, A.; Belanzoni, P.; Bellachioma, G.; Zuccaccia, C.; Zuccaccia, D.; Macchioni, A., *Green Chem.* **2011,** *13*, 3360–3374.
105. Grotjahn, D. B.; Brown, D. B.; Martin, J. K.; Marelius, D. C.; Abadjian, M.-C.; Tran, H. N.; Kalyuzhny, G.; Vecchio, K. S.; Specht, Z. G.; Cortes-Llamas, S. A.; Miranda-Soto, V.; van Niekerk, C.; Moore, C. E.; Rheingold, A. L., *J. Am. Chem. Soc.* **2011,** *133*, 19024–19027.
106. Zuccaccia, C.; Bellachioma, G.; Bolaño, S.; Rocchigiani, L.; Savini, A.; Macchioni, A., *Eur. J. Inorg. Chem.* **2012,** *2012*, 1462–1468.
107. Hong, D.; Murakami, M.; Yamada, Y.; Fukuzumi, S., *Energy Environ. Sci.* **2012,** *5*, 5708–5716.
108. Wang, C.; Wang, J.-L.; Lin, W., *J. Am. Chem. Soc.* **2012,** *134*, 19895–19908.
109. Hintermair, U.; Sheehan, S. W.; Parent, A. R.; Ess, D. H.; Richens, D. T.; Vaccaro, P. H.; Brudvig, G. W.; Crabtree, R. H., *J. Am. Chem. Soc.* **2013,** *135*, 10837–10851.
110. Blakemore, J. D.; Mara, M. W.; Kushner-Lenhoff, M. N.; Schley, N. D.; Konezny, S. J.; Rivalta, I.; Negre, C. F. A.; Snoeberger, R. C.; Kokhan, O.; Huang, J.; Stickrath, A.; Tran, L. A.; Parr, M. L.; Chen, L. X.; Tiede, D. M.; Batista, V. S.; Crabtree, R. H.; Brudvig, G. W., *Inorg. Chem.* **2013,** *52*, 1860–1871.
111. Codolà, Z.; M. S. Cardoso, J.; Royo, B.; Costas, M.; Lloret-Fillol, J., *Chem. - Eur. J.* **2013,** *19*, 7203–7213.
112. Graeupner, J.; Hintermair, U.; Huang, D. L.; Thomsen, J. M.; Takase, M.; Campos, J.; Hashmi, S. M.; Elimelech, M.; Brudvig, G. W.; Crabtree, R. H., *Organometallics* **2013,** *32*, 5384–5390.
113. Zuccaccia, C.; Bellachioma, G.; Bortolini, O.; Bucci, A.; Savini, A.; Macchioni, A., *Chem. - Eur. J.* **2014,** *20*, 3446–3456.
114. Savini, A.; Bucci, A.; Bellachioma, G.; Rocchigiani, L.; Zuccaccia, C.; Llobet, A.; Macchioni, A., *Eur. J. Inorg. Chem.* **2014,** *2014*, 690–697.
115. Ingram, A. J.; Wolk, A. B.; Flender, C.; Zhang, J.; Johnson, C. J.; Hintermair, U.; Crabtree, R. H.; Johnson, M. A.; Zare, R. N., *Inorg. Chem.* **2014,** *53*, 423–433.
116. Thomsen, J. M.; Sheehan, S. W.; Hashmi, S. M.; Campos, J.; Hintermair, U.; Crabtree, R. H.; Brudvig, G. W., *J. Am. Chem. Soc.* **2014,** *136*, 13826–13834.
117. Zhang, T.; deKrafft, K. E.; Wang, J.-L.; Wang, C.; Lin, W., *Eur. J. Inorg. Chem.* **2014,** *2014*, 698–707.
118. Lewandowska-Andralojc, A.; Polyansky, D. E.; Wang, C.-H.; Wang, W.-H.; Himeda, Y.; Fujita, E., *Phys. Chem. Chem. Phys.* **2014,** *16*, 11976–11987.
119. Wan, X.; Wang, L.; Dong, C.-L.; Menendez Rodriguez, G.; Huang, Y.-C.; Macchioni, A.; Shen, S., *ACS Energy Lett.* **2018,** *3*, 1613–1619.
120. Dzik, W. I.; Calvo, S. E.; Reek, J. N. H.; Lutz, M.; Ciriano, M. A.; Tejel, C.; Hetterscheid, D. G. H.; de Bruin, B., *Organometallics* **2011,** *30*, 372–374.
121. Brewster, T. P.; Blakemore, J. D.; Schley, N. D.; Incarvito, C. D.; Hazari, N.; Brudvig, G. W.; Crabtree, R. H., *Organometallics* **2011,** *30*, 965–973.
122. Schley, N. D.; Blakemore, J. D.; Subbaiyan, N. K.; Incarvito, C. D.; D'Souza, F.; Crabtree, R. H.; Brudvig, G. W., *J. Am. Chem. Soc.* **2011,** *133*, 10473–10481.
123. Blakemore, J. D.; Schley, N. D.; Kushner-Lenhoff, M. N.; Winter, A. M.; D'Souza, F.; Crabtree, R. H.; Brudvig, G. W., *Inorg. Chem.* **2012,** *51*, 7749–7763.

124. Hintermair, U.; Hashmi, S. M.; Elimelech, M.; Crabtree, R. H., *J. Am. Chem. Soc.* **2012,** *134*, 9785–9795.
125. Junge, H.; Marquet, N.; Kammer, A.; Denurra, S.; Bauer, M.; Wohlrab, S.; Gärtner, F.; Pohl, M.-M.; Spannenberg, A.; Gladiali, S.; Beller, M., *Chem. - Eur. J.* **2012,** *18*, 12749–12758.
126. Diaz-Morales, O.; Hersbach, T. J. P.; Hetterscheid, D. G. H.; Reek, J. N. H.; Koper, M. T. M., *J. Am. Chem. Soc.* **2014,** *136*, 10432–10439.
127. Hetterscheid, D. G. H.; van der Ham, C. J. M.; Diaz-Morales, O.; Verhoeven, M. W. G. M.; Longo, A.; Banerjee, D.; Niemantsverdriet, J. W.; Reek, J. N. H.; Feiters, M. C., *Phys. Chem. Chem. Phys.* **2016,** *18*, 10931–10940.
128. Abril, P.; del Rı́o, M. P.; Tejel, C.; Verhoeven, T. W. G. M.; Niemantsverdriet, J. W. H.; van der Ham, C. J. M.; Kottrup, K. G.; Hetterscheid, D. G. H., *ACS Catal.* **2016,** *6*, 7872–7875.
129. Corbucci, I.; Ellingwood, K.; Fagiolari, L.; Zuccaccia, C.; Elisei, F.; Gentili, P. L.; Macchioni, A., *Catal. Today* **2017,** *290*, 10–18.
130. Materna, K. L.; Crabtree, R. H.; Brudvig, G. W., *Chem. Soc. Rev.* **2017,** *46*, 6099–6110.
131. Zhang, L.; Cole, J. M., *ACS Appl. Mater. Interfaces* **2015,** *7*, 3427–3455.
132. Love, J. C.; Estroff, L. A.; Kriebel, J. K.; Nuzzo, R. G.; Whitesides, G. M., *Chem. Rev.* **2005,** *105*, 1103–1170.
133. Pinson, J.; Podvorica, F., *Chem. Soc. Rev.* **2005,** *34*, 429–439.
134. Blakemore, J. D.; Gupta, A.; Warren, J. J.; Brunschwig, B. S.; Gray, H. B., *J. Am. Chem. Soc.* **2013,** *135*, 18288–18291.
135. Dogutan, D. K.; McGuire, R.; Nocera, D. G., *J. Am. Chem. Soc.* **2011,** *133*, 9178–9180.
136. Smits, N. W. G.; den Boer, D.; Wu, L.; Hofmann, J. P.; Hetterscheid, D. G. H., *Inorg. Chem.* **2019,** *58*, 13007–13019.
137. Jackson, M. N.; Surendranath, Y., *Acc. Chem. Res.* **2019,** *52*, 3432–3441.
138. van der Ham, C. J. M.; Işık, F.; Verhoeven, T. W. G. M.; Niemantsverdriet, J. W.; Hetterscheid, D. G. H., *Catal. Today* **2017,** *290*, 33–38.
139. Rossi, L. M.; Fiorio, J. L.; Garcia, M. A. S.; Ferraz, C. P., *Dalton Trans.* **2018,** *47*, 5889–5915.
140. Kunz, S., *Top. Catal.* **2016,** *59*, 1671–1685.
141. Chung, Y.-H.; Chung, D. Y.; Jung, N.; Sung, Y.-E., *J. Phys. Chem. Lett.* **2013,** *4*, 1304–1309.
142. Zhou, Z.-Y.; Kang, X.; Song, Y.; Chen, S., *J. Phys. Chem. C* **2012,** *116*, 10592–10598.
143. Elgrishi, N.; Rountree, K. J.; McCarthy, B. D.; Rountree, E. S.; Eisenhart, T. T.; Dempsey, J. L., *J. Chem. Educ.* **2018,** *95*, 197–206.
144. Martin, D. J.; McCarthy, B. D.; Rountree, E. S.; Dempsey, J. L., *Dalton Trans.* **2016,** *45*, 9970–9976.
145. Costentin, C.; Drouet, S.; Robert, M.; Savéant, J.-M., *J. Am. Chem. Soc.* **2012,** *134*, 11235–11242.
146. Rountree, E. S.; McCarthy, B. D.; Eisenhart, T. T.; Dempsey, J. L., *Inorg. Chem.* **2014,** *53*, 9983–10002.
147. Costentin, C.; Savéant, J.-M., *ChemElectroChem* **2014,** *1*, 1226–1236.
148. Costentin, C.; Savéant, J.-M., *J. Am. Chem. Soc.* **2017,** *139*, 8245–8250.
149. Hetterscheid, D. G. H., *Chem. Commun.* **2017,** *53*, 10622–10631.
150. Bullock, R. M.; Appel, A. M.; Helm, M. L., *Chem. Commun.* **2014,** *50*, 3125–3143.
151. Bard, A. J.; Faulkner, L. R., *Electrochemical Methods: Fundamentals and Applications*. Wiley: New York, 2000.
152. Zhou, R.; Zheng, Y.; Jaroniec, M.; Qiao, S.-Z., *ACS Catal.* **2016,** *6*, 4720–4728.
153. Kottrup, K. G.; D'Agostini, S.; van Langevelde, P. H.; Siegler, M. A.; Hetterscheid, D. G. H., *ACS Catal.* **2018,** *8*, 1052–1061.
154. Langerman, M.; Hetterscheid, D. G. H., *Angew. Chem. Int. Ed.* **2019,** *58*, 12974–12978.
155. Li, M.; Takada, K.; Goldsmith, J. I.; Bernhard, S., *Inorg. Chem.* **2016,** *55*, 518-526.
156. Hessels, J.; Yu, F.; Detz, R.; Reek, J., *ChemSusChem* **2020,** *in press*.
157. D'Agostini, S. Mechanistic studies of the water oxidation reaction with molecular iron catalysts. PhD dissertation, Leiden University, Leiden, 2020.
158. Yi, Y.; Weinberg, G.; Prenzel, M.; Greiner, M.; Heumann, S.; Becker, S.; Schlögl, R., *Catal. Today* **2017,** *295*, 32–40.
159. Benck, J. D.; Pinaud, B. A.; Gorlin, Y.; Jaramillo, T. F., *PLoS One* **2014,** *9*, e107942.
160. van Dijk, B.; Hofmann, J. P.; Hetterscheid, D. G. H., *Phys. Chem. Chem. Phys.* **2018,** *20*, 19625–19634.
161. Sauerbrey, G., *Z. Phys.* **1959,** *155*, 206–222.
162. Deakin, M. R.; Melroy, O., *J. Electroanal. Chem. Interfacial Electrochem.* **1988,** *239*, 321-331.
163. Kanazawa, K. K.; Gordon, J. G., *Anal. Chem.* **1985,** *57*, 1770–1771.
164. Buttry, D. A.; Ward, M. D., *Chem. Rev.* **1992,** *92*, 1355–1379.